Durham E-Theses

Detailed studies of mid-ocean ridge volcanism at the Mid-Atlantic Ridge (45N) and elsewhere

YEO, ISOBEL,ALICE,L

How to cite:

YEO, ISOBEL,ALICE,L (2012) *Detailed studies of mid-ocean ridge volcanism at the Mid-Atlantic Ridge (45N) and elsewhere*, Durham theses, Durham University. Available at Durham E-Theses Online: http://etheses.dur.ac.uk/4944/

Use policy

The full-text may be used and/or reproduced, and given to third parties in any format or medium, without prior permission or charge, for personal research or study, educational, or not-for-profit purposes provided that:

- a full bibliographic reference is made to the original source
- a link is made to the metadata record in Durham E-Theses
- the full-text is not changed in any way

The full-text must not be sold in any format or medium without the formal permission of the copyright holders.

Please consult the full Durham E-Theses policy for further details.

Academic Support Office, The Palatine Centre, Durham University, Stockton Road, Durham, DH1 3LE
e-mail: e-theses.admin@durham.ac.uk Tel: +44 0191 334 6107
http://etheses.dur.ac.uk

Formation of volcanic crust at slow-spreading mid-ocean ridges by steady-state processes

B. J. Murton[a], N. Schroth[a], T. LeBas[a], P. van Calsteren[b], I. Yeo[c], K. Achenbach[c] and R. C. Searle[c]

[a] National Oceanography Centre, Empress Dock, Southampton SO14 3ZH, UK

[b] Department of Earth and Environmental Sciences, The Open University, Milton Keynes, MK7 6AA, UK

[c] Department of Earth Sciences, Durham University, Durham DH1 3LE, UK

Introduction:

Mid-ocean ridges (MORs) dominate the global magmatic flux and generate 61% of the Earth's crust. Three quarters are slow-spreading (<40mm/year) and characterised by prominent axial volcanic ridges (AVRs) that focus volcanic crustal accretion[1,2]. Previous studies suggest AVRs are episodic on a time scale of 150-300 ka[3,4,5,6,7]. This, however, is paradoxical as AVRs occur at nearly all known slow-spreading MOR segments[8,9,10,11,12]. Here, we test this paradox by presenting a detailed study of a well-developed AVR at 45°N on the Mid-Atlantic Ridge (MAR). This location is typical of slow-spreading MORs: spreading symmetrically and orthogonally (at a full rate of 22.1 mm/yr[13]), having a deep axial valley and robust AVR[14,15,16,17], Figure 1A). By combining bathymetry, sidescan sonar, visual mapping and geochemistry we conclude that AVRs are not episodic but instead are steady-state volcanotectonic features of crustal accretion at slow-spreading MORs. From our data, we show how a low but nearly continuous flux of melt builds the AVR while simultaneously its flanks subside and are buried by episodic high-melt flux eruptions. This process involves two distinct sources of magma: one, producing normal mid-ocean ridge basalt (N-MORB), is located beneath the AVR; the other, producing enriched E-MORB, is located off-axis beneath the median valley floor where it potentially drives hydrothermal circulation and mineralisation on the ridge flanks.

Main:

One of the most striking features of slow-spreading MOR segments is the nearly ubiquitous presence of a prominent and elevated AVR surrounded by the low-lying seafloor of the median valley. For example, AVRs occur in fourteen out of eighteen well-mapped segments along the MAR between 24° to 31°N[11,18,19,20]; they are associated with rough hummocky terrain compared to smoother seafloor covering the median valley floor.

At 45°N (MAR) this change from hummocky AVR to smoother seafloor covering the median valley and uplifted ridge flanks is clearly demonstrated by a high-frequency roughness map (Figure 1B). Generated from multibeam bathymetry, using a 5x5 (450 m by 450 m) high-pass filter followed by a 3x3 standard deviation filter to isolate the high-frequency hummocky morphology, the map shows a typical root-mean square roughness for the AVR of 31 m (average peak-to-trough amplitude of 62 m for the hummocks).

The roughness of the AVR reflects its formation by ~3000 small volcanic cones with an average volume of ~0.001 km^3 [17]. These result from frequent, short-lived, small volume, eruptions of pillow lava[17] that have extruded vertically from the crest and flanks of the AVR. Occasionally, the summits of the hummocky volcanic cones are capped with 10-15 m high pinnacles of basalt with slopes of ~60°. Together, these volcanic features indicate slow effusion rates (<1 m^3 per second)[21,22] and are consistent with low eruption pressures due to a close balance between magma pressure and the hydrostatic head of the column of melt supplying the AVR[23,24]. Using the maximum elevation of the AVR above the median valley floor of 450 m, average densities for basaltic magma of 2.7±0.04 g cm^{-3} [25] and for mafic crust of 2.9 g cm^{-3} [26] and a hydrostatic eruptive model[23], we estimate a depth of between 5.4 km and 8.1 km to the top of melt bodies located beneath the AVR (i.e. at or near the base of the crust[27]).

In contrast to the hummocky AVR, the low-lying median valley floor and uplifted ridge flanks form smoother terrain (Figure 1B) with an average peak-to-trough amplitude of 16 m. The median valley floor is covered in massive lava flows with only a thin (<0.5 m thick) veneer of sediment. Where exposed, these massive lavas include multi-layered, ropey textured sheet-flows, each up to several metres thick (Figure 1C), indicative of rapid eruption rates of 100s of m^3 per second[21,22]. Some of these sheet-flows (e.g. at the north-eastern end of the ridge segment) appear to originate from flat-topped seamounts that are exclusive to the smooth floors of the median valley and axial flanks (Figure 1D). Elsewhere, exposed high-up in the fault scarps forming the median valley walls, massive lava flows of up to several metres thick overlay pillow lavas (Figure 1E).

Since AVRs are the main locus of crustal accretion[1,2], the reduction in seafloor roughness implies burial of the hummocky AVR flanks beneath the smoother floor of the median valley. Sedimentation rates here are ~5cm per thousand years[28] yielding an average sediment thickness of less than 1 m, even at a distance of 6 km from the AVR crest. Also, sediment at the top of the rift valley walls was observed by the ROV Isis to be less than 2 m thick. Hence an accumulation of sediment alone cannot bury the hummocky flanks of the AVR. This, instead, requires a cumulative thickness of at least 46 m for the massive lava flows that cover the median valley floor.

Compared with the AVR, the relatively large volumes and long run-out lengths of the massive lava flows burying the flanks of the AVR and covering the median valley floor require more rapid effusion rates[21]. For example, assuming an effusion rate of 100m^3 per second[21,22], the 0.03 to 0.06 km^3 volume for the north-eastern sheet-flow would have taken between 3.5 and 7 days to erupt. These rapid eruptions indicate higher magma pressures [23,24] and lower viscosities for melt sourced from deep and possibly hot reservoirs located several kilometres off-axis under the outer-margins of the median valley floor.

Burial of the AVR beneath the median valley floor implies subsidence of its flanks. High-resolution bathymetry profiles across the AVR at 45°N reveal a number of outward-facing scarps on both its eastern and western flanks that dip at >45° (Figure 1F). These scarps subdivide the flanks of the AVR into a series of linear terraces, several hundreds of metres long, that progressively step down towards the smooth and flat-lying median valley floor creating a structural horst. Some of the upper-surfaces of the terraces dip gently backwards towards the centre of the AVR, consistent with back-rotation by shallow-rooted normal faults. Visual observations reveal these as high-angle AVR-parallel fault scarps, a few tens of metres high with broken pillow lavas forming steep cliffs (Figure 1G). Elsewhere, the faults are inferred from outward-facing scarps that are partially draped by younger lavas (Figure 1H). The maximum accumulated throw for these outward facing faults, measured from the profiles, is 260 m accommodating 50% of the subsidence of the AVR flanks. Hence the AVR is as much a tectonic feature as it is a volcanic edifice and, as such, the accretionary axis of slow-spreading MORs behaves in a similar way to the rise crest of fast-spreading MORs[29].

The contrast between the AVR hummocky lavas and median valley floor massive lavas is reflected compositionally. While both have overlapping Cr and Ni concentrations, indicating similar degrees of fractional crystallisation (Figure 2A), they show a bi-modal distribution of incompatible trace element concentrations (Figure 2B) indicating derivation from different primary melts and discrete magma bodies. The majority of AVR pillow-lavas form a group that has lower concentrations and ratios of incompatible trace elements (i.e. N-MORB) compared with the enriched compositions (i.e. E-MORB) of the massive-flows and flat-topped volcanoes of the median valley floor (e.g. lower Zr for a given Y: Figure 2B). Some flat-topped seamounts also have compositions that are nearly identical to their adjacent massive sheet-flows indicating a close affinity between them.

Discussion:

The E-MORB composition of the massive lavas covering the median valley floor and the flat-topped seamounts could indicate derivation from a lower degrees of partial mantle melting. By comparison, the N-MORB composition of the hummocky AVR pillow lavas could indicate derivation from a higher degree of partial mantle melting. Assuming bulk partition coefficients for Zr and Nb during mantle melting are close to zero, the ~22% difference in Zr between the average AVR lava and that of the enriched group corresponds to a ~20% reduction in melt fraction for the median valley floor magmas. The equivalent change in Nb concentrations is ~66%, indicating a ~60% reduction in melt fraction. Since this is impossible for a homogeneous source, we propose that the E-MORB lavas are derived from a heterogeneous mantle that is both enriched in highly incompatible trace elements and melted to a smaller degree compared with the N-MORB AVR hummocky flows. At lower degrees of partial mantle melting the magma composition is strongly influenced by the preferential addition of melts from more fusible heterogeneities (e.g. streaks of eclogite and/or pyroxenite)[30]. These melts enrich the E-MORB magmas that supply both the flat-topped volcanoes and the median valley floor sheet-flows. Larger melt fractions dilute these enrichments and yield a more continuous supply of N-MORB magma to the AVR.

Eruption of different parental magma compositions require discreet magma reservoirs, located both on-axis beneath the AVR and several kilometres off-axis beneath the median valley floor, with separate melt pathways to the seafloor resulting in little opportunity for melt homogenisation prior to eruption. Magma bodies located beneath the median valley floor, that episodically erupt sheet-flows, can also supply heat to form off-axis hydrothermal venting and seafloor massive sulphides away from the AVR crest[31] and even on axial valley walls[32]. This bi-modal volcanic distribution is remarkably similar to fast spreading MORs where recent seismic imaging has shown off-axis (by 3-6km) melt lenses[33] that supply E-MORB magmas to flat-topped seamounts and ridge-flank lavas while on-axis melt lenses supply N-MORB magmas to volcanic accretion at the rise crest[34]. Hence there appear to be similar spatial scales of magma heterogeneity and focusing from the melt zone beneath both fast and slow-spreading MORs.

Conclusions:

In contrast to previous models describing a cyclic evolution for AVRs, we propose that AVRs are the product of frequent, small-volume, moderate-melt fraction, low-effusion rate eruptions of pillow lavas at their crest and continuous subsidence of their flanks. These are buried by episodic, large volume, low-melt fraction, fast-effusion rate eruptions of massive lavas that cover the median valley floor (Figure 3). Variations in the flux and frequency of eruptions result in interleaving of AVR flanks with massive-flows erupting across the median valley floor. Hence there is no cyclicity per se for the AVR and no paradox for their near ubiquitous presence throughout all slow-spreading MORs. In this scheme, the AVR behaves like a glacier, accreting new material (i.e. lava) across the top while simultaneously it flanks spread and subside (i.e. by faulting) towards its base. In both its tectonic and magmatic processes, the behaviour of slow-spreading MORs is much more similar to fast-spreading MORs than previously thought.

Acknowledgments:

This work was funded by the Natural Environment Research Council through grants awarded to Murton (at the National Oceanography Centre) and Searle (at the University of Durham: awards NE/ C520612/1 & NE/C520598/1). We are also indebted to the professionalism and enthusiasm of the officers and crew, the shipboard scientific party, and the shipboard and ROV technical teams, of the RRS James Cook (cruise JC024).

References:

1. Macdonald, K. C. Mid-Ocean Ridges: Fine sale tectonic, volcanic and hydrothermal processes within the Plate Boundary Zone, Annual Rev. Earth Planet. Sci., 10, 155-189 (1982)

2. Grindlay, N. R., Fox, P. J. & Macdonald, K. C. Second-order ridge axis discontinuities in the South Atlantic: Morphology, structure, and evolution, *Marine Geophys. Res.*, **13**, 21-49 (1991)

3. Parson, L. M. et al. En echelon axial volcanic ridges at the Reykjanes Ridge: a life cycle of volcanism and tectonics. *Earth Planet Sci. Lett.*, **117**, 73-87 (1993)

4. Murton, B. J. & Parson, L. M. Segmentation, volcanism and deformation of oblique spreading centres: a quantitative study of the Reykjanes Ridge. *Tectonophysics*, **222**, 237-257 (1993)

5. Gente, P. et al. Characteristics and Evolution of the Segmentation of the Mid-Atlantic Ridge Between 20° N and 24° N During the Last 10 Million Years, *Earth Planet Sci. Lett.*, **129**, 55–71 (1995)

6. Peirce, C. & Sinha, M. Life and death of axial volcanic ridges: Segmentation and crustal accretion at the Reykjanes Ridge. *Earth Planet Sci. Lett.*, **274**, 112–120 (2008)

7. Thatcher, W. & Hill, D. P. A simple model for the fault-generated morphology of slow-spreading mid-ocean ridges. *Jour. Geophys. Res.*, **100**, 561-570 (1995)

8. Ballard, R. D. & van Andel, Tj. H. Morphology and tectonics of the inner rift valley at lat 36°50'N on the Mid-Atlantic Ridge, *Geol. Soc. Am. Bull.*, **88**, 507–530 (1977)

9. Brozena, J. & Chayes, D. A Sea Beam Study of the Mid-Atlantic Ridge, 15°–17° S, *Eos, Trans., Amer. Geophys. Union*, **69**, 1494 (1988)

10. Keeton, J.A., Searle, R.C., Parsons, B., White, R. S., Murton, B. J., Parson, L. M., Peirce, C., Sinha, M. C. Bathymetry of the Reykjanes Ridge. *Marine Geophys. Res.*, **19**, 55–64 (1997)

11. Briais, A., Sloan, H., Parson L. M. & Murton B. J. Accretionary processes in the median valley of the Mid-Atlantic Ridge 27 N–30°N from TOBI side-scan sonar images. *Marine Geophys. Res.*, **21**, 87–119 (2000)

12. Raju, K. A. K., Chaubey, A. K., Amarnath, D., Mudholkar, A. Morphotectonics of the Carlsberg Ridge between 62°20' and 66°20'E, Northwest Indian Ocean, *Marine Geology*, **252**, 120-128 (2008)

13. DeMets, C., Gordon, R. G., Argus, D. F. & Stein, S. Effect of recent revisions to the geomagnetic reversal time scale on estimate of current plate motions, *Geophys. Res. Lett.*, **21**, 2191-2194 (1994)

14. Schafer, C. T. The Mid-Atlantic Ridge Near 45 °N. XXII. Sedimentary Deposition and Lithogenesis on Mid-Atlantic Ridge Mountain Tops. *Can. J. Earth Sci.*, **11**, 1157–1167 (1974)

15. Searle, R.C., et al. Structure and development of an Axial Volcanic Ridge: Mid-Atlantic Ridge, 45°N, *Earth Planet. Sci. Lett.*, **299**, 228-241 (2010)

16. Shaw, P. R. Ridge segmentation, faulting and crustal thickness in the Atlantic Ocean, *Nature*, **358**, 490-493 (1992)

17. Yeo, I., Searle, R. C., Achenbach, K. L., Le Bas, T. P. & Murton B. J. Eruptive hummocks: Building blocks of upper-oceanic crust. *Geology*, **40**, 91-94 (2012)

18. Purdy, G. M., Sempere, J. C., Schouten, H., Dubois, D. L. & Goldsmith, R. Bathymetry of the Mid-Atlantic Ridge, 24°–31°N. *Mar. Geophys. Res*., **12**, 247 – 252 (1990)

19. Smith, D. K., Cann, J. R., Dougherty, M. E. et al. Mid-Atlantic Ridge volcanism from deep-towed side-scan sonar images, 25°–29°N. *J. Volc. Geotherm. Res*., **67**, 233–262 (1995)

20. Smith, D. K., Tivey, M. A., Schouten, H. & Cann, J. R. Tracking the active spreading axis along 80 km of the Mid-Atlantic Ridge, *J. Geophys. Res*., **104**, 7599-7612 (1999)

21. Gregg, T. K. P. & Fink, J. H. Quantification of submarine lava-flow morphology through analogue experiments. *Geology*, **23**, 73-76 (1995)

22. Griffiths, R. W. & Fink, J. H. Solidification and morphology of submarine lavas: A dependence on extrusion rate, *J. Geophys. Res*., **97**, 19,729–19,737 (1992)

23. Smith, D. K. & Cann, J. R. Building the crust at the Mid-Atlantic Ridge, *Nature*, **365**, 707–715 (1993)

24. Head, J. W., III., Wilson, L. & Smith, D. K. Mid-ocean ridge eruptive vents: Evidence for dike widths, eruption rates, and evolution of eruptions and axial volcanic ridges, *J. Geophys. Res.*, **101**, 28,265–28,280 (1996)

25. Sakamaki, T., Urakawa, S., Suzuki, A., Ohtani, E., Katayama, Y. Density Measurement for MORB Melts by X-ray Absorption Method. *American Geophys. Union, Fall Meeting 2006,* MR43C-1104 (2006)

26. Carlson, R. L. & Raskin, G. S. Density of the ocean crust. *Nature*, **311**, 555-558 (1984)

27. Keen, C. & Tramontini, C. A Seismic Refraction Survey on the Mid-Atlantic Ridge. *Geophys J. Royal Astro. Soc.*, **20**, 473-491 (1970)

28. Keen, M.J. & Manchester, K.S. The Mid-Atlantic Ridge near 45°N. Sediment distribution and thickness from seismic reflection profiling, Canada. J*. Earth Sci.,* **7**, 735-747 (1970)

29. Carbotte, S. M., Macdonald, K. C. The axial topographic high at intermediate and fast spreading ridges. *Earth Planet. Sci. Lett.*, **128**, 85-97 (1994)

30. Mello, S. L. M., Cann, J. R., Fowler, C. M. R. Anomalous mantle at 45°N Mid-Atlantic Ridge? *J. Geophys. Res. Solid Earth*, **104**, 29335–29349 (1999)

31. Rona P. A., Klinkhammer, G., Nelsen, T.A., Trefry, J.H., Elderfield, H. Black smokers, massive sulphides and vent biota at the Mid-Atlantic Ridge: *Nature*, **321**, 33–37 (1986)

32. Hashimoto, J., et al. First hydrothermal vent communities from the Indian Ocean discovered: *Zoological Science*, **18**, 717–721 (2001)

33. Canales, J. P., et al., Network of off-axis melt bodies at the East Pacific Rise. *Nature Geoscience*, doi:10.1038/ngeo1377 (2012)

34. Perfit, M. R. et al. Small-scale spatial and temporal variations in mid-ocean ridge crest magmatic processes. *Geology*, **22**, 375–379 (1994)

Figures:

Figure 1. Composite figure showing key geological and geophysical observations of the AVR: A) EM120 swath sonar bathymetry, gridded at 50m and hill-shaded from the NE of the segment at 45°N, showing the positions of inset figures 1C-F. B) Roughness map (derived from the bathymetry) shows the AVR is dominated by hummocky terrain while the median valley floor and flanks of the Mid-Atlantic Ridge are mainly smooth. C) Photograph (3 m x 4 m) showing a massive sheet on the floor of the median valley. D) Detail of sidescan sonar imagery showing a massive sheet flow (bright backscatter, outlined in yellow) covering part of the floor of the median valley. E) Photograph (2 m x 3 m) showing a massive lava flow at least 1.5 m-thick exposed near the top of the western median valley wall. F) High-resolution bathymetry profile across the AVR, obtained from the TOBI vehicle (see figure 1 for location). The profile shows steep slopes related to linear scarps that trend N-S and face down the flank of the AVR. These are interpreted as outward-facing normal faults on the hummocky flanks of the AVR generating a horst structure for the AVR. On the median valley walls, the scarps are inward facing, generating a graben structure. The profile also shows the difference between the hummocky AVR topography and the smooth and flat-lying seafloor of the median valley. Symbols denote: (pl) pillow lavas, (sf) sheet flows, (AVR) axial volcanic ridge, (MVF) median valley floor, (RF) rift flank. G) Composite image (3m x by 8 m) showing a westward-facing fault scarp of brecciated pillow-lavas cutting the western flank of the AVR. H) Photograph (2m x 3m) showing lavas draped over a near vertical, outward facing scarp interpreted as part of an outward facing fault.

Figure 2. Key geochemical indicators of magmatic fractionation and source variation. Symbols: Blue filled diamonds are hummocky terrain forming the main body of the AVR; green filled triangles are hummocky terrain forming a spur on the north-eastern flank of the AVR; red filled squares are massive sheet flows filling the median valley floor; yellow filled squares are flat-topped volcanoes on the median valley floor. All trace-element analyses were made on pressed powder pellets from whole-rocks, determined by wavelength

dispersive XRF. Analytical errors are less than the size occupied by the figure symbols. A) Cr vs. Ni co-variation diagram for lavas from the 45°N segment. All groups overlap in Cr vs. Ni space indicating no systematic differences in the extent of crystal fractionation. B) Zr vs. Y co-variation: There are two clear groups of volcanic compositions within the 45°N segment of the Mid-Atlantic Ridge: the hummocky terrain of the AVR (forming a lower Zr group) and the median valley massive-flows and seamounts (forming a higher Zr group). These differences indicate derivation of the lavas from different parental melts. Oval fields enclose flat-topped volcanoes and spatially adjacent sheet flow lavas of similar composition indicating cogenesis.

Figure 3. Cartoon (not to scale) showing the essential elements of the steady-state AVR process: large melt-fraction magmas segregate from the centre of the asthenospheric melting zone and supply N-MORB to magma chambers (mc) located beneath the AVR. Small melt-fraction magmas from the periphery of the melting zone supply E-MORB to magma chambers located under the median valley floor. The AVR magmas frequently erupt small volumes of pillow lava (pl) building an elevated ridge of hummocky volcanic mounds. Simultaneously, the flanks of the AVR subside toward the median valley floor where less frequent but larger volume eruptions of E-MORB bury the hummocky terrain of the AVR beneath sheet flows (sf).


A
B
C
D
E
F
G
H
45°42'0"N
45°36'0"N
45°30'0"N
45°24'0"N
28°0'0"W
27°54'0"W
27°48'0"W
27°42'0"W
Depth (m)
1000
1400
1800
2200
2600
3000
3400
3800
Kilometres
5
0
2 SD (m)
0
8
12
18
24
30
1 km
20/06/08 05:46.40
ALT 003 HDG 117
DEP 2825
DOP 004
500 m
RF
sf
MVF
sf
sf
pl
AVR
pl
pl
MVF
sf
sf
sf

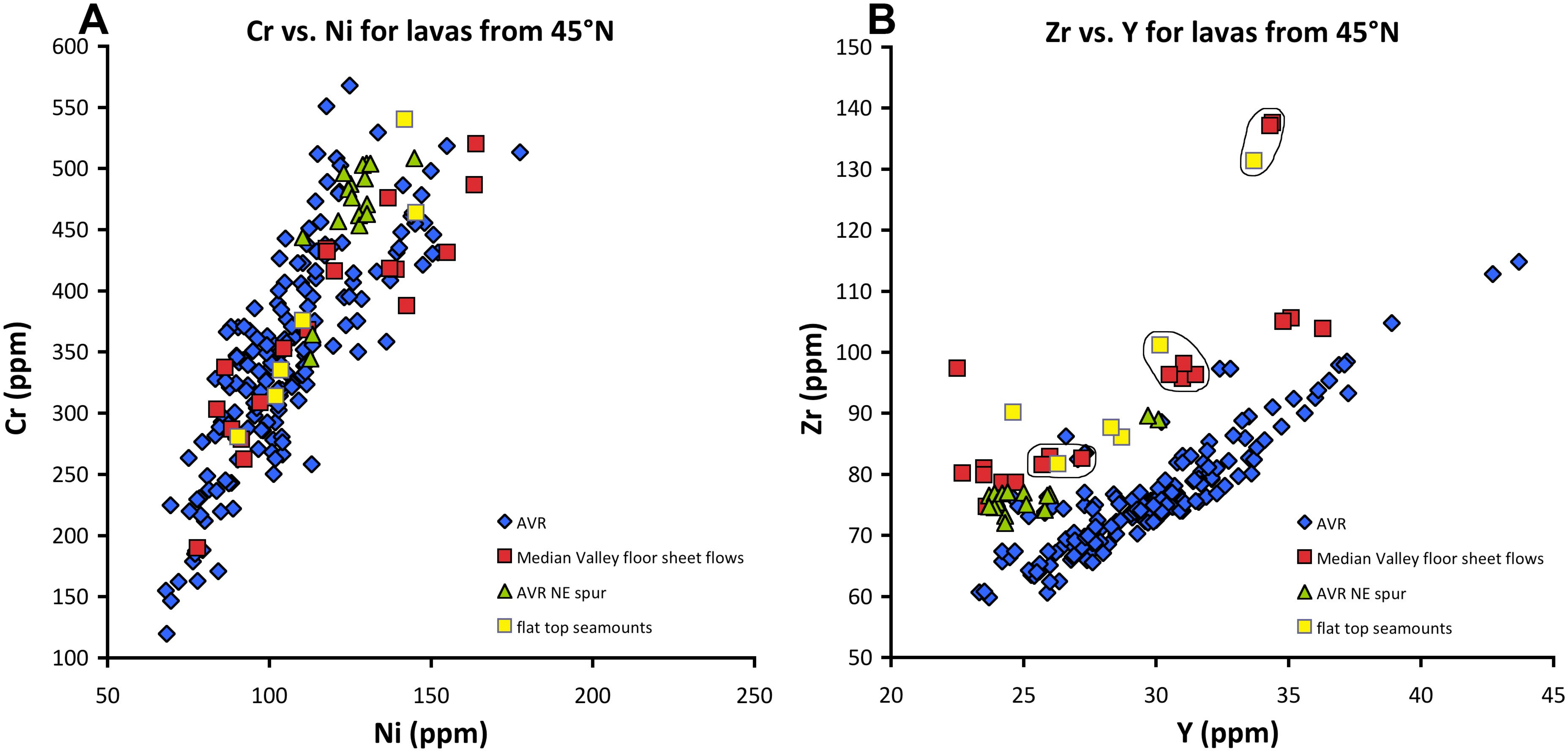
A
Cr vs. Ni for lavas from 45°N
Cr (ppm)
600
550
500
450
400
350
300
250
200
150
100
Ni (ppm)
50
100
150
200
250
AVR
Median Valley floor sheet flows
AVR NE spur
flat top seamounts
B
Zr vs. Y for lavas from 45°N
Zr (ppm)
150
140
130
120
110
100
90
80
70
60
50
Y (ppm)
20
25
30
35
40
45
AVR
Median Valley floor sheet flows
AVR NE spur
flat top seamounts

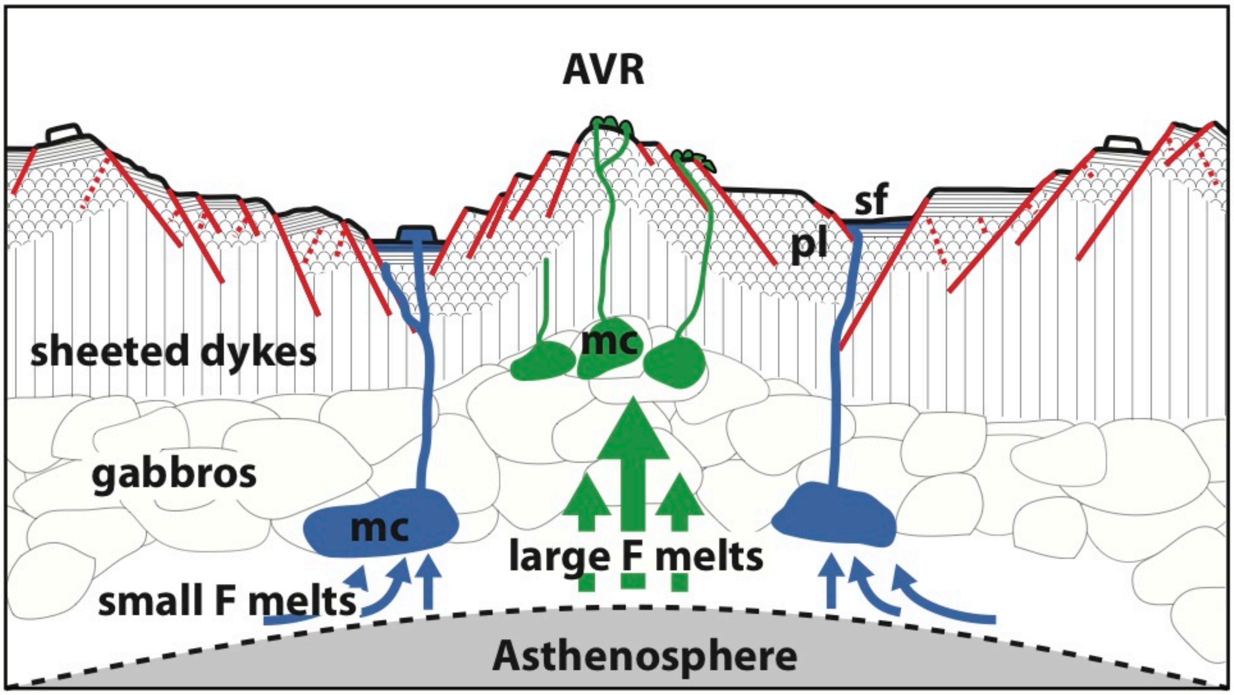
AVR
sf
pl
sheeted dykes
mc
gabbros
mc
large F melts
small F melts
Asthenosphere